

Spin-flop transition in manganese fluoride subjected to a tilted magnetic field. Tricritical point in the H - ψ diagram

V. V. Eremenko, N. É. Kaner, Yu. G. Litvinenko, and V. V. Shapiro

Physicotechnical Institute of Low Temperatures, Academy of Sciences of the Ukrainian SSR, Kharkov
(Submitted 25 March 1985)

Zh. Eksp. Teor. Fiz. **89**, 1289–1300 (October 1985)

Optical spectroscopy was used to study in detail the orientational magnetic phase transitions in an MnF_2 crystal in a magnetic field inclined at an angle to the tetragonal axis in (010) and $(1\bar{1}0)$ planes. An investigation was made of the dynamics of reorientation of the antiferromagnetic vector as a function of the field intensity, tilt angle ψ , and geometry of the tilt of \mathbf{H} . In the $\mathbf{H}\|C_4$ configuration the antiferromagnetic vector was oriented in the basal plane along $[100]$ in fields $\mathbf{H} > H_c$. The sign and magnitude of the fourth-order anisotropy constant were determined in that plane. It was found that the H - ψ phase diagram had a tricritical point when the vector \mathbf{H} was tilted in the $(1\bar{1}0)$ plane.

1. INTRODUCTION

Manganese fluoride is the most thoroughly investigated two-sublattice antiferromagnet exhibiting the easy-axis anisotropy. Its Néel temperature is 68 K, the crystal structure is tetragonal, and the symmetry group is D_{4h}^{14} . Figure 1 shows a magnetic unit cell of MnF_2 .

In an external magnetic field parallel to the spontaneous ordering axis C_4 this compound exhibits a first-order magnetic orientational phase transition in which the antiferromagnetic vector \mathbf{l} abruptly switches to the basal plane and this is known as the spin-flopping transition. The transition is manifested by a jump in the longitudinal magnetization in a magnetic field $H_c \approx 9.5$ T (Refs. 1 and 2). When the field \mathbf{H} is inclined to the tetragonal axis, the magnitude of the jump of the antiferromagnetic vector decreases and disappears when the angle reaches $\psi_{cr} = 30^\circ$ (Ref. 2). This critical angle ψ_{cr} is governed by the ratio of the axial anisotropy field $H_A \sim 0.8$ T to the exchange interaction field $H_E = 54$ T, and the critical field of the transition is given by $H_c \approx (2H_E H_A)^{1/2}$. These results are in good agreement with theoretical calculations^{3,4} carried out ignoring the anisotropy in the basal plane.

However, the magnetic susceptibility measurements² have failed to yield the orientation of the vector \mathbf{l} in the spin-flop phase. The magnetization in the basal plane was found to be practically isotropic in tilted magnetic fields.

The orientation of the antiferromagnetic vector in the basal plane of the spin-flop phase is governed, when the field orientation is along the C_4 axis, by the magnetic anisotropy energy in this plane. This may be either the fourth-order anisotropy $f l_x^2 l_y^2$ or the second-order anisotropy $d(l_x m_y + l_y m_x)$, corresponding to the Dzyaloshinskii interaction.¹⁾ Here, x and y are selected along the $[100]$ and $[010]$ axes (Fig. 1). Calculations⁵ show that when the parameter f is negative, the vector \mathbf{l} is oriented along the two-fold diagonal axis $[110]$. For a positive f , the direction of the antiferromagnetic vector depends on the relationship between the parameters f and d : if $d < d_0 \propto (Af)^{1/2}$, the vector \mathbf{l} is parallel to the $[100]$ direction, whereas for $d > d_0$, it is oriented along $[110]$. Here, A is the exchange interaction parameter.

The characteristic features of the spin-flop transition in a magnetic field have been investigated earlier also by spectroscopic methods.^{6,7} A usual splitting of the exciton absorption line of frequency $31\,938\text{ cm}^{-1}$ of the ${}^6A_{1g}({}^6S) - {}^4T_{1g}({}^4P)$ transition in magnetic fields $H > H_c$ was reported in Ref. 6, but could not be explained. A later investigation⁷ was concerned with the anisotropy of the splitting of this exciton line in the case of a larger tilt angle $\psi = 19^\circ$ in a field $H = 13.2$ T. However, it was assumed in Ref. 7 that the magnetic anisotropy in the basal plane was so strong that the component of the antiferromagnetic vector \mathbf{l}_1 in the basal plane of the spin-flop phase is always oriented along the $[110]$ axis irrespective of the direction of the transverse component of the field \mathbf{H}_1 in this plane. This hypothesis⁷ is in conflict with the experimental results obtained in our study.⁸ We demonstrated that a tilt of the magnetic field by 3° or more from the C_4 axis makes the vector \mathbf{l}_1 always parallel to \mathbf{H}_1 . Therefore, the conclusion reached in Ref. 7 that the component \mathbf{l}_1 is always directed along the $[110]$ axis is incorrect.

The absorption of ultrasound in MnF_2 was investigated by Melcher⁹ near the phase transition to the spin-flop phase at frequencies close to that of the soft mode of the antiferromagnetic resonance. In the absence of anisotropy in the basal plane this mode is activation-free, but a finite energy gap appears because of the anisotropy energy in the basal plane,

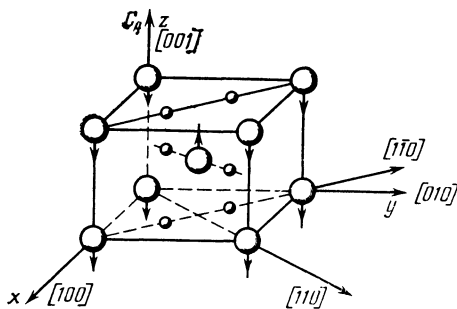


FIG. 1. Unit magnetic cell of the antiferromagnet MnF_2 . The large circles represent the Mn^{2+} ions and the small circles are the F^- ions.

particularly because of the fourth-order anisotropy. A magnetoacoustic resonance appears because of the magnetoelastic coupling which mixes acoustic vibrations with spin oscillations. Melcher⁹ investigated abrupt changes in the elastic constants in the spin-flop transition field and used a comparison with theoretical formulas given in another of his papers¹⁰ to reach the conclusion that the anisotropy constant f was negative. Hence, Melcher postulated that the antiferromagnetic vector of the spin-flop phase was oriented along the [110] axis. However, the formulas for the magnetoelastic interaction used in Ref. 9 were incorrect, like the conclusion about the orientation of \mathbf{l}_1 along [110].

We carried out a detailed experimental study of the characteristic features of the orientational phase transitions in MnF_2 subjected to tilted magnetic fields and this was done for various geometries of the tilt of the vector \mathbf{H} away from the tetragonal axis. We used optical spectroscopy based on the explicit dependence of the splitting of the above-mentioned exciton line on the field intensity, angle of tilt of the field relative to the C_4 axis, and orientation of the vector \mathbf{l}_1 , which in turn also depends on the first two factors. This method has the undoubted advantage that the frequencies of the spectral lines affected by the phase transition are not influenced by the macroscopic magnetic structure of the samples, particularly by the presence of domains if these domains are not of the 90° type.

In Sec. 2 we shall describe briefly the features of the experimental method. In Sec. 3 we shall report and discuss the results of the experimental determination of the orientation of \mathbf{l}_1 in the basal plane. The magnitude of the anisotropy constant will be deduced in Sec. 4 from the experimental data. In Sec. 5 we shall analyze the dynamics of reorientation of the antiferromagnetic vector in the spin-flop phase as a function of the intensity of the magnetic field and the geometry of its tilt away from the C_4 axis. Finally, in Sec. 6, we shall discuss the phase diagram in terms of the field intensity and the tilt angle as the coordinates, and demonstrate the existence of a tricritical point and formulate conclusions.

2. EXPERIMENTAL METHOD

The optical absorption spectrum of an antiferromagnetic MnF_2 crystal was investigated using pulsed magnetic fields of up to 16 T intensity. The fields were generated in a compact solenoid (internal channel diameter 10 mm) cooled with liquid nitrogen. The field rose to its maximum value in 2 msec. A special system was developed for locating and moving a sample inside the solenoid and this made it possible to determine very accurately the orientation of the tetragonal axis of the crystal and to measure its tilt relative to the magnetic field. The apparatus was designed to determine the dependence of the frequency of an exciton-magnon band at $28\,027\text{ cm}^{-1}$ of the ${}^6A_{1g}({}^6S)-{}^4T_{2g}({}^4D)$ transition on the magnetic field in the case of spin flopping.¹¹

Figure 2 shows the behavior of the frequency of this band and of the ${}^6A_{1g}({}^6S)-{}^4T_{1g}({}^4P)$ exciton line of frequency $31\,938\text{ cm}^{-1}$ on the intensity of the external magnetic field in the vicinity of the spin-flop transition when the field was oriented exactly along the C_4 axis. It is clear from this

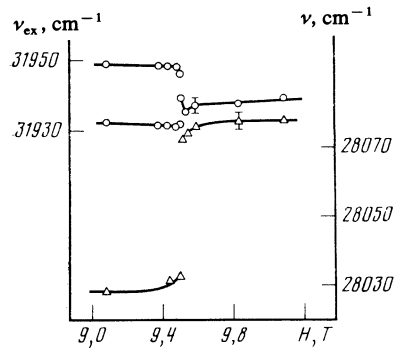


FIG. 2. Dependences of the frequencies of the Zeeman doublet of the ν_{ex} exciton line due to the ${}^6A_{1g}({}^6S)-{}^4T_{1g}({}^4P)$ transition (left-hand scale, \circ), and of the exciton-magnon band ν due to the ${}^6A_{1g}({}^6S)-{}^4T_{2g}({}^4D)$ transition (right-hand scale, \triangle), on the intensity of an external magnetic field H in the vicinity of the transition to the spin-flop phase in the case when the vector \mathbf{H} is exactly parallel to the C_4 axis ($\psi = 0$).

figure that in the spin-flop field H_c the frequencies of both bands exhibited a jump. Figure 3 shows the dependences of the frequencies of the band and line on the field intensity in the case when the field was tilted by an angle of $\psi = 50^\circ$ in the (010) plane away from the tetragonal axis. In this case the spin-flop transition was extended on the field scale: it occurred in an interval of fields which was the same for both the exciton-magnon band and the exciton line, and the dependence of the frequency of the exciton-magnon band reproduced, to a certain scale, the dependence of the longitudinal magnetization on H (continuous curve joining the points represented by Δ).

When the external magnetic field was oriented exactly along the tetragonal axis of the crystal, the absorption was measured at a frequency intermediate between its limiting values before and after the spin-flop transition. When the tilt angle ψ did not exceed 30° , there was no absorption of light at this intermediate frequency. At higher values of the angle ψ when the dependence of the frequency of the exciton-magnon band on the field intensity was smooth, the absorption signal at the intermediate frequency spread into a curve with a maximum when the field was increased during a pulse.

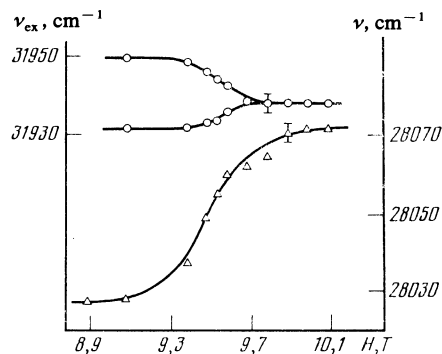


FIG. 3. Dependences of the frequencies of the Zeeman doublet of the exciton line ν_{ex} (left-hand scale, \circ) and of the exciton-magnon band ν (right-hand scale, \triangle), and of the longitudinal magnetization (continuous curve passing through the points \triangle , arbitrary scale) on the magnetic field H tilted at an angle of $\psi = 50^\circ$ in the (010) plane.

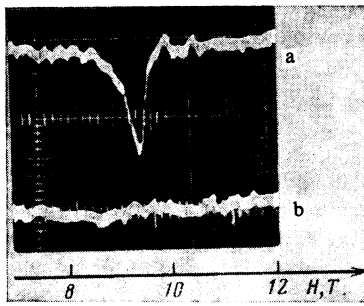


FIG. 4. Optical transmission oscillograms at the frequency $28\,052\text{ cm}^{-1}$ at $T = 14\text{ K}$: a) $\psi = 1.5^\circ$; b) $\psi = 0$.

Figure 4b shows oscillograms obtained at the frequency of $28\,052\text{ cm}^{-1}$ for $\psi = 0$ (Fig. 4b) and $\psi = 1.5^\circ$ (Fig. 4a).

We used a DFS-8 spectrograph with a linear dispersion of 3 \AA/mm . Beyond the exit slit of the spectrograph we placed a photomultiplier which produced a signal applied to an oscilloscope. Micrometric screws were used to rotate the sample relative to the solenoid axis. These screws made it possible to alter the angle ψ within the range $0\text{--}3^\circ$ and the error in the determination of this angle did not exceed $5'$. The position of the sample was monitored by a laser beam. The reflections of this beam from two mirrors attached rigidly to the sample and to the solenoid were displayed on a screen and this made it possible to determine the tilt angle of the field away from the tetragonal axis, as well as the direction of the component of the magnetic field in the basal plane of the crystal (angle Φ). When the measurements were made at high values of the angle ψ (from 3 to 12°) and in strong magnetic fields up to 25 T , the sample was located in the solenoid channel by means of calibrated quartz wedges and such a setting was accurate to within $20'$. Therefore, in each series we carried out a control measurement at $T = 14\text{ K}$. However, in each series there was a control point at 4.2 K . We found no difference between the experimental results obtained at 14 and 4.2 K .

3. EXPERIMENTAL RESULTS AND DISCUSSION

Figure 5 shows the dependence of the splitting of the $31\,938\text{ cm}^{-1}$ exciton line on the tilt angle of the field away from the tetragonal axis in the (110) plane, obtained for different values of the field intensity ($10.5, 12, 15.5\text{ T}$). The

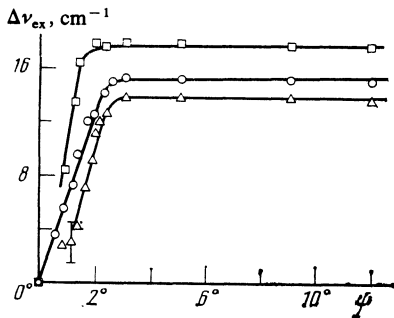


FIG. 5. Dependences of the splitting of the exciton line ν_{ex} on the angle ψ for different values of the field H tilted in the (110) plane: \square) 10.5 T ; \circ) 12 T ; \triangle) 15.5 T .

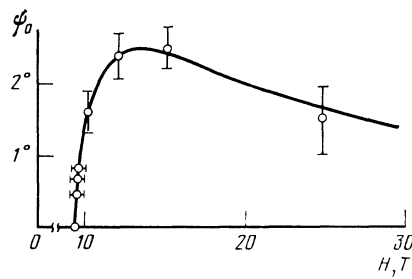


FIG. 6. Dependences of the angle ψ_0 on the magnetic field H in the (110) plane; the continuous curve is calculated.

magnitude of the splitting $\Delta\nu_{\text{ex}}$ increased on increase in the angle ψ only up to a certain limit. Beginning from the angle ψ_0 , which depended on the field intensity, the splitting remained constant, at least in the interval $\psi_0 < \psi < 12^\circ$. The magnitude of the characteristic angle ψ_0 first increased on increase in the field and then fell. Figure 6 illustrates the dependence of ψ_0 on H . It should be pointed out that when the field was tilted in the (010) plane there was no splitting of the exciton line in fields $H > H_c$ and for all values of ψ , at least in the range from 0 to 12° .

The absence of the splitting in the $\psi = 0$ case and when the field tilt was in the (010) plane, on the one hand, and the splitting in the case of the tilt in the (110) plane, on the other, led us to the firm conclusion that the antiferromagnetic vector was in the basal plane after transition to the spin-flop phase when the field was oriented exactly along the C_4 axis. The vector \mathbf{l} was directed along the two-fold axis $[100]$ or $[010]$ axis. Moreover, we concluded that this orientation of the vector \mathbf{l} was due to the fourth-order anisotropy with an energy $f l_x^2 l_y^2$ and a positive constant f . When the magnetic field was tilted away from the tetragonal axis in the (110) plane, the energy of the interaction between the magnetic moments of the sublattices with the magnetic field began to compete with the fourth-order magnetic anisotropy energy. As a result of this competition the antiferromagnetic vector began to rotate on increase in the angle ψ : the rotation was in the basal plane from the $[100]$ to the $[110]$ axis and this corresponded to the rising parts of the curves in Fig. 5. When the tilt angle reached $\psi > \psi_0(H)$, the transverse component of the antiferromagnetic vector \mathbf{l}_\perp became parallel to the transverse component of the field \mathbf{H}_\perp (horizontal parts of the curves in Fig. 5).

4. ESTIMATES OF THE FOURTH-ORDER ANISOTROPY CONSTANT

The experimental dependences of the splitting of the exciton line on the angle ψ ($\mathbf{H}_\perp \parallel [110]$) enabled us to estimate the order of magnitude of the anisotropy constant f . This could be done by deriving a theoretical expression for the magnitude and H -dependence of the characteristic angle $\psi_0(H)$. We shall use the Hamiltonian of a uniaxial two-sublattice antiferromagnet^{3,4} and include the term corresponding to the fourth-order anisotropy:

$$\mathcal{H} = \frac{A}{2} m^2 + \frac{a}{2} m_z^2 + \frac{b}{2} l_z^2 + f l_x^2 l_y^2 - \mathbf{m} \cdot \mathbf{h}. \quad (1)$$

Here,

$$A > 0, \quad f > 0, \quad b < 0, \quad a + b < 0,$$

where $A = 4M_0 H_E$ is the exchange interaction parameter; $b = -2M_0 H_A$; a and b are the axial magnetic anisotropy constants; M_0 is the modulus of the magnetization density of the sublattices; $h = 2M_0 \mathbf{H}$; $\mathbf{m} = (\mathbf{M}_1 + \mathbf{M}_2)/2M_0$ is the ferromagnetic vector; $\mathbf{l} = (\mathbf{M}_1 - \mathbf{M}_2)/2M_0$ is the antiferromagnetic vector; \mathbf{M}_i are the sublattice magnetizations.

Since the value of ψ is small, we shall assume that the parameter f is small compared with the exchange interaction A and axial anisotropy b constants. The Hamiltonian (1) must be minimized with respect to the angles θ and Φ , where θ is the angle between the direction of \mathbf{l} and the C_4 axis, and Φ is the angle between \mathbf{l}_1 and $[100]$. In magnetic fields much higher than the critical value and for small values of f the angle θ corresponding to the absolute minimum of the Hamiltonian (1) can be replaced quite accurately with θ corresponding to the minimum of this Hamiltonian when the term $f^2 l_x^2 l_y^2$ is omitted. In this case it is convenient to use the results of Ref. 12, where manganese fluoride is regarded as a uniaxial antiferromagnet with an isotropic basal plane. The equilibrium values of the angles between the C_4 axis and the magnetizations of the sublattices of MnF_2 in tilted magnetic field are calculated in Ref. 12 for the case when the tilt angle exceeds the critical value ψ_{c1} and the phase transition does not occur. An allowance for just the axial anisotropy with $b < 0$ and neglect of the basal plane anisotropy has the effect that the antiferromagnetic and ferromagnetic vectors are oriented in the same plane as the field and the C_4 axis. Therefore, using the results of Ref. 12 we shall automatically exclude from consideration the $\mathbf{l}_1 \perp \mathbf{m}_1 \parallel \mathbf{H}_1$ phase, which may appear in the interval between the noncoplanar and coplanar $\mathbf{l}_1 \parallel \mathbf{m}_1 \parallel \mathbf{H}_1$ phases. Such a phase is unusual for antiferromagnets with the axial anisotropy of the easy axis type and it may appear precisely because of the basal plane anisotropy. The substitution of the equilibrium value of θ gives an expression for the Hamiltonian (1) which depends only on the angle Φ . Dropping the terms that do not contain a dependence on Φ yields

$$\mathcal{H}(\Phi) = \frac{H_{A4}}{4} \left(1 - \frac{H^2}{4H_E^2} \right)^2 \times \left[\sin^2 2\Phi - \frac{2^{1/2} H^4 \psi^2 (\sin \Phi + \cos \Phi)}{H_E H_{A4} (H^2 - H_c^2 - H_A^2) (1 - H^2/4H_E^2)} \right]. \quad (2)$$

Here, a characteristic fourth anisotropy field $H_{A4} = f/2 M_0$ is included. Minimization of Eq. (2) with respect to the angle Φ shows that the solution corresponding to $\mathbf{l}_1 \parallel \mathbf{H}_1 \parallel [110]$ has the lowest energy if

$$\psi > \psi_0(H) \approx 2(1/H^2 - 1/4H_E^2) [H_E H_{A4} (H^2 - H_c^2 - H_A^2)]^{1/2}. \quad (3)$$

An analysis of this solution shows that the function $\Phi = \Phi_{\min}(\psi, H)$, corresponding to the minimum of Eq. (2), exhibits a kink of the line $\psi_0(H)$ in its dependence on ψ , i.e., its first derivative $\Phi'_{\min}(\psi)$ with respect to the angle ψ exhibits a finite jump. It follows that the $\psi_0(H)$ line represents a second-order phase transition.

It is clear from Eq. (3) that in the interval between H_c

and H_E the function $\psi_0(H)$ is nonmonotonic. Using the experimental value of $\psi_0 = 2.5^\circ$ corresponding to $H = 12 T$ (Fig. 5), we find that $H_{A4} \approx 32 \times 10^{-4} T$. A similar estimate for the fields 10.5 and 15.5 T gives a similar value of H_{A4} .

In the range of fields from 11 to 20 T the change in ψ_0 is slight and it amounts to $\approx 10\%$ (Fig. 5). There is a good agreement between the experimental values of ψ_0 and those calculated from Eq. (3) (Fig. 6). The maximum of the $\psi_0(H)$ curve occurs at $H \approx 2^{1/2} H_c$ and the value of ψ at the maximum is estimated to be $(H_{A4}/2H_A)^{1/2}$.

As pointed out in the Introduction, the orientation of the vector \mathbf{l} along the $[100]$ axis in the spin-flop phase corresponds not only to a positive value of the constant f , but also to the condition $d < d_0 \propto (Af)^{1/2}$. Consequently, the following estimate for the upper limit can be obtained for the effective Dzyaloshinskii interaction field in MnF_2 :

$$H_D = d/2M_0 < H_D^0 \approx (H_E H_{A4})^{1/2} \sim 10^{-1} T.$$

5. ANALYSIS OF THE DYNAMICS OF THE ANTIFERROMAGNETIC VECTOR ON APPLICATION OF A MAGNETIC FIELD TILTED FROM THE TETRAGONAL AXIS

In this section we shall discuss and compare with calculations the experimental data on the splitting of the exciton line, which can be used to determine the orientation of the antiferromagnetic vector in the basal plane, and the change in this orientation as a function of the magnetic field intensity for different geometries of the tilt of this field away from the fourfold axis.

1. Tilt of the magnetic field in the (010) plane

This geometry corresponds to curve 1 in Fig. 7 and the experimental points are denoted by black dots. The calculated curve and the experimental results correspond to the tilt angle $\psi = 50^\circ$. It is shown in Sec. 2 that after the transition to

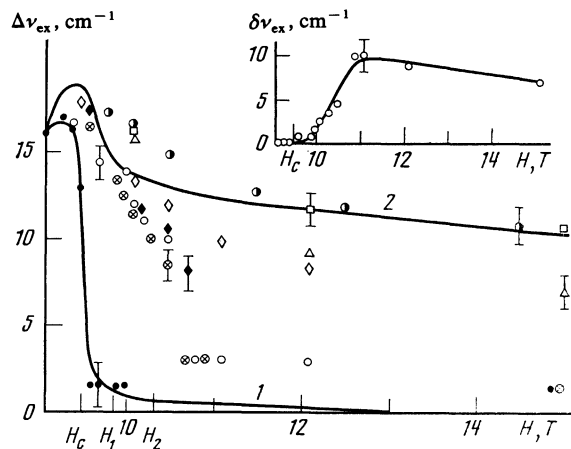


FIG. 7. Comparison of the calculated and experimental values of the splitting of the exciton line, plotted as a function of the magnetic field for different tilt angles ψ : 1) 2) calculated for $\psi = 50^\circ$: 1) vector \mathbf{H} in the (010) plane; 2) vector \mathbf{H} in the (110) plane; \bullet - $\psi = 50^\circ$; $\mathbf{H}_1 \parallel [100]$. All the other experimental points were obtained for $\mathbf{H}_1 \parallel [110]$: \circ $\psi = 26^\circ$, \blacklozenge $\psi = 40^\circ$; \otimes $\psi = 30^\circ$; \circ $\psi = 2^\circ$; \triangle $\psi = 1.5^\circ$; \diamond $\psi = 1.15^\circ$. The inset shows the difference between the calculated (curve 2) and experimental ($\psi < 50^\circ$) data, plotted as a function of the magnetic field.

the spin-flop phase when the field is exactly parallel to the tetragonal axis, the antiferromagnetic vector is oriented along [110]. The tilt of the field in this plane does not disturb the coplanar nature of all three vectors \mathbf{H} , \mathbf{l} , and \mathbf{m} , i.e., the component \mathbf{l}_\perp is parallel to the [100] binary axis. It is clear from Fig. 7 that the experimental points lie quite close to the calculated curve 1. The calculations were carried out using formulas given in our earlier paper⁸ on the assumption that $\mathbf{l}_\perp \parallel \mathbf{H}_\perp$. The good agreement between the experimental results and the calculations provides further support for the conclusion that the vectors \mathbf{l} , \mathbf{m} , and \mathbf{H} are coplanar and lie in the (010) plane.

2. Tilt of the magnetic field in the (1 $\bar{1}$ 0) plane at $\psi = 3^\circ$

In this geometry the field dependence of the splitting of the exciton line is quite different from that in the preceding case (points denoted by \bullet in Fig. 7). The splitting remains finite, at least up to fields of 25 T. As shown in Sec. 3 (Fig. 5), in the geometry under discussion and for the selected tilt angle ψ the component of the antiferromagnetic vector in the basal plane \mathbf{l}_\perp is now parallel to \mathbf{H}_\perp . An additional proof of the correctness of this conclusion is provided by the good agreement between the experimental results and the calculations of the splitting of the exciton line.⁸ The magnitude of the splitting is governed by the Dzyaloshinskii-Moriya interaction in an excited state:

$$\Delta\nu_{\text{ex}}(H) \approx D_f S_f^2 (\sin^2 \vartheta_1 + \sin^2 \vartheta_2), \quad (4)$$

where D_f is the constant of the second-order uniaxial anisotropy in the basal plane for the excited ${}^4T_{1g}$ (4P) state; S_f is the spin of an excited ion; ϑ_1 and ϑ_2 are the angles between the spins of the excited ions belonging to different sublattices and the tetragonal axis. These angles are different and they slowly decrease on increase in the field intensity. It should be stressed that Eq. (4) is obtained in Ref. 8 on the assumption that $\mathbf{l}_\perp \parallel \mathbf{H}_\perp \parallel [110]$. The experimental results fit well the calculated curve. It follows that once again, as in the case of the field tilt in the (010) plane, all the three vectors \mathbf{H} , \mathbf{l} , and \mathbf{m} are coplanar, but they are now in the (1 $\bar{1}$ 0) plane.

3. Small tilt of the vector \mathbf{H} in the (1 $\bar{1}$ 0) plane

When the angle of tilt of the magnetic field in the (1 $\bar{1}$ 0) plane is small, the situation is more complex and dynamic. This is due to the fact that the vector \mathbf{l}_\perp corresponding to $\psi = 0$ in the spin-flop phase is always directed along the [100] axis, whereas for large angles ψ it is directed along [110] (in this geometry). Therefore, clearly at low angles ψ the vectors \mathbf{l} , \mathbf{H} , and \mathbf{m} are not coplanar.

Curve 2 in Fig. 7 represents the results of a calculation of the splitting of the exciton line carried out using the formulas given in Ref. 8 for the case when $\psi = 50^\circ$ and the magnetic field is oriented in the (110) plane. Calculations are based on the assumption, as in the $\psi > 2.5^\circ$ case, that $\mathbf{l}_\perp \parallel \mathbf{H}_\perp \parallel [110]$. It is clear from Fig. 7 that the bulk of the experimental points corresponding to several values of the tilt angle (26', 40', 50') obtained in fields $H > 10$ T lie far from the calculated curve. The inset in Fig. 7 illustrates the field dependence of $\delta\nu_{\text{ex}}$ representing the difference between the calculated (curve 2) and experimental (for the angles

$\psi < 50^\circ$) values of the splitting $\Delta\nu_{\text{ex}}$. The curve in the inset joins the experimental points.

The initial parts of the field dependences of the splitting agree (within the limits of the experimental error) with the theoretical curve 2 for all tilt angles. Significant deviations of the experimental data from the calculations begin directly beyond a critical field H_c , when the transition to the spin-flop phase has already occurred, but as the field intensity is increased, the sublattice moments gradually become aligned with the field.

For $\psi > 1^\circ$ the splitting does not disappear on increase in the magnetic field intensity, but it is considerably less than the calculated value. As the tilt angle ψ approaches 2.5° , the differences between the experimental and calculated splitting decreases rapidly. Only some of the experimental points obtained in the range $\psi > 1^\circ$ are plotted in Fig. 7 in order not to overload the figure.

At the end of Sec. 3 the nature of the angular dependences of the splitting of the exciton line (Fig. 5) in the selected geometry of the tilt of the magnetic field ($H > H_c$) is used to draw the conclusion that the component of the antiferromagnetic vector in the basal plane becomes reoriented from the [100] to the [110] axis on increase in the angle ψ . This means that for the tilt angles of the magnetic field in the (110) plane smaller than 2.5° the three vectors \mathbf{H} , \mathbf{l} , and \mathbf{m} are no longer coplanar. In other words, the process of reorientation of the magnetic sublattices is affected strongly by the fourth-order anisotropy. Additional support for the conclusion that the vectors \mathbf{H} , \mathbf{l} , and \mathbf{m} are not coplanar is provided in this case by our dependences of the splitting on the field intensity and orientation, and by the differences between the observed values of the splitting and those calculated on the assumption that $\mathbf{l}_\perp \parallel \mathbf{H}_\perp \parallel [110]$.

In the whole of the preceding analysis we have essentially allowed only for the fourth-order anisotropy $f_x^2 l_y^2$ in the basal plane. However, in addition to this anisotropy, there are also effects due to the second-anisotropy corresponding to the Dzyaloshinskii interaction $d(l_x m_y + l_y m_x)$. As already pointed out, this interaction tends to lock the antiferromagnetic vector in the basal plane along the [110] axis. An allowance for the second-order anisotropy makes it possible to understand some features of the behavior of the splitting of the exciton line in the spin-flop phase when the magnetic field is tilted through a small angle ($\psi < 50^\circ$) in the (1 $\bar{1}$ 0) plane.

In fact, the fourth-order anisotropy is proportional to l_\perp^4 and it has the strongest influence on the dynamics of a reorientation of the antiferromagnetic vector component in the basal plane in the range of fields where l_\perp is maximal. This occurs when the magnetization vectors of each of the sublattices form angles θ_α close to $\pi/2$ ($\alpha = 1$ and 2 are the sublattice numbers). Figure 7 gives the values of the field intensities H_1 and H_2 , for the tilt angles $\psi = 25$ and 50° , respectively, which correspond to $\theta_\alpha = \pi/2$. As the field is increased compared with such values of H , the role of the fourth-order anisotropy decreases rapidly, whereas the influence of the component \mathbf{H}_\perp on the establishment of the orientation $\mathbf{l}_\perp \parallel \mathbf{H}_\perp \parallel [110]$ should increase. Therefore, in this situation we can expect the vector \mathbf{l}_\perp to become aligned along

the $[110]$ axis and the line splitting to increase. However, the experiments demonstrate precisely the opposite behavior: the splitting does not increase on increase in H but decreases, i.e, the vector \mathbf{l}_1 continues to tilt away from the direction of \mathbf{H}_1 . In all probability this is due to the Dzyaloshinskii interaction. In the range of fields $H > H_c$ where the experimental values of the splitting agree with the calculations carried out for $\mathbf{l}_1 \parallel [110]$, we can probably expect two orthogonal magnetic configurations which depend on the ratio of the second- and fourth-order anisotropy parameters d and f . One of them corresponds to the orientation $\mathbf{l}_1 \parallel [110] \parallel \mathbf{H}_1$ and the other to the antiferromagnetic vector \mathbf{l}_1 , which is parallel to the other $[1\bar{1}0]$ axis and is perpendicular to \mathbf{H}_1 . However, spectroscopic methods based on the dependence of the splitting of the exciton line on the orientation of \mathbf{l}_1 cannot be used readily to distinguish these two orthogonal configurations from one another (because in both cases \mathbf{l}_1 is oriented along the diagonal axis and the splitting $\Delta\nu_{\text{ex}}$ is approximately the same). Which of these configurations (or those close to them) is realized in MnF_2 crystals and for which angles and magnetic field intensities can be determined by appropriate theoretical calculations and a comparison with the experimental results.

The proposed description of the dynamics of reorientation of the antiferromagnetic vector in the spin-flop phase under the action of a magnetic field tilted relative to the tetragonal axis makes it possible to explain in a natural manner the experiments² in which the magnetic susceptibility was measured. It was established in Ref. 2 that the magnetic susceptibility of MnF_2 crystals shows no anisotropy in the basal plane when the field is tilted at angles of $\psi = 10$ and 20° . This observation has not been explained satisfactorily even allowing for the existence of a domain structure in the spin-flop phase. The appearance of two orthogonal configurations with $\mathbf{l}_1 \parallel [110] \parallel \mathbf{H}_1$ and $\mathbf{l}_1 \parallel [110] \perp \mathbf{H}_1$ in the basal plane under the action of a tilted magnetic field in the $(1\bar{1}0)$ plane should make the transverse magnetization practically isotropic even after allowance for the magnetic anisotropy effects in the basal plane.

6. PHASE DIAGRAM OF THE FIELD INTENSITY AGAINST THE TILT ANGLE. TRICRITICAL POINT. CONCLUSIONS

In this section we shall discuss the nature of the phase transition in the antiferromagnet MnF_2 when the spin-flopping of the magnetic sublattices in a magnetic field occurs for different directions of the tilt of this field relative to the tetragonal axis. According to earlier theoretical calculations^{3,4} and the experimental data,² the transition to the spin-flop phase is of the first order not only for $\psi = 0$ but also for small tilt angles $\psi < \psi_{c1} = 30^\circ$. Figure 8a shows the angular dependence of the field of the transition to the spin-flop phase when the magnetic field is tilted in the (010) plane and it illustrates this conclusion. The first-order phase transition line terminates at a critical point where the antiferromagnetic and spin-flop phases become indistinguishable.

Figure 8b shows the H - ψ phase diagram obtained for MnF_2 when the field is tilted in the $(1\bar{1}0)$ plane. The curve in Fig. 8b separates the H - ψ plane into two regions. In one of

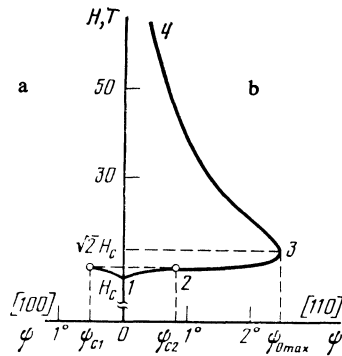


FIG. 8. Phase diagram plotted using the H - ψ coordinates: a) \mathbf{H} in the (100) plane; b) \mathbf{H} in the $(1\bar{1}0)$ plane.

them, to the right of the curve, the MnF_2 crystal behaves as a uniaxial antiferromagnet with an isotropic basal plane when subjected to a tilted magnetic field and the vectors \mathbf{l} , \mathbf{m} , and \mathbf{H} are coplanar. To the left of the curve the basal plane anisotropy plays an important role and makes the vectors \mathbf{H} , \mathbf{l} , and \mathbf{m} noncoplanar. The interval 1-2 in the phase diagram represents the first-order phase transition line,^{3,4} like the curve in Fig. 8a. After passing through the interval 1-2 the antiferromagnetic vector becomes oriented in the basal plane and its direction is close to $[100]$. The part of the phase diagram 2-3-4 represents a curve described by Eq. (3) (compare with Fig. 6) and is a second-order phase transition line. The conclusion that the 2-3-4 line is not a first-order phase transition line follows, in addition to the analysis made in Sec. 4, from all the available experimental data for the appropriate values of the angles ψ and H . In other words, the function $\mathbf{l}_1(H, \psi)$ should be continuous on the phase transition line and singularities may be exhibited only by the derivatives of this function. In any case, the jumps in the orientation of the antiferromagnetic vector and the splitting of the exciton line were not observed within the limits of the experimental error.

Clearly, the first-order phase transition line 1-2 should merge with the second-order phase transition line at some value of the angle ψ_{c2} , corresponding to the field $H_{c1} = (H_c^2 + H_A^2)^{1/2}$. It therefore follows that the point 2 should be regarded as tricritical where the first- and second-order phase transition lines meet after arrival from the opposite sides of the same point. We shall refer to the point of intersection of the lability boundary line with the second-order phase transition line as the tricritical point (which is in agreement with the current terminology). The value of the angle ψ_{c2} may generally be different from $\psi_{c1} = 30^\circ$ at which the first-order phase transition line terminates in the $\mathbf{H}_1 \parallel [100]$ geometry (Fig. 8a). In fact, it is clear from the experimental data in Fig. 7 that the dependences of the splitting of the exciton line on the magnetic field intensity in the $\mathbf{H} \parallel (110)$ geometry practically coincide with one another for all the angles $\psi = 25$ - 50° , i.e., they are practically independent of ψ . On the other hand, if $\psi > 1^\circ$, then the nature of the dependence of the splitting on the magnetic field begins to vary rapidly on increase in ψ approaching the dependence calculated for the case when $\mathbf{l}_1 \parallel [110]$. This clearly shows

that the value of the angle ψ_{c2} differs from 30° and reaches $50 \pm 10^\circ$ in the $\mathbf{H} \parallel (1\bar{1}0)$ geometry.

It should be pointed out that an allowance for the second-order anisotropy corresponding to the Dzyaloshinskii interaction not only does not alter the proposed pattern of the orientational magnetic phase transitions in MnF_3 , but just the opposite: it gives grounds regarding these conclusions as more reliable and permanent. This applies particularly to the stability of the state with $\mathbf{l}_1 \parallel [110]$ in the $\mathbf{H} \parallel (1\bar{1}0)$ geometry, because the second-order anisotropy tends to align the antiferromagnetic vector along the $[110]$ axis. Naturally, when an allowance is made for this anisotropy the phase curve becomes deformed and this effect increases on increase in the magnetic field intensity.

Our investigations thus yielded the following main results.

1. An anisotropy of the splitting of the exciton line was established and it was used to identify the positive sign of the constant f of the fourth-order anisotropy in the basal plane of the antiferromagnet MnF_2 and to determine its value $H_{A4} \approx 32 \times 10^{-4} T$.

2. It was shown experimentally that when the external magnetic field was precisely parallel to the tetragonal axis of the crystal, the antiferromagnetic vector became oriented as a result of the spin-flop transition in the basal plane along the $[100]$ axis.

3. The experiments in tilted magnetic fields were used to construct the phase diagram of the antiferromagnet MnF_2 in

terms of the magnetic field intensity and the tilt angle. It was found that in the $\mathbf{H} \parallel (100)$ geometry the curve representing the first-order phase transitions terminates at a critical point and in the $\mathbf{H} \parallel (1\bar{1}0)$ geometry the phase transition lines have a tricritical point separating the regions of the curves representing the first- and second-order phase transitions.

¹⁾We have omitted some of the fourth-order terms permitted by the symmetry, but unimportant from the point of view of their role in the investigated effect and resulting in most cases only in renormalization of the constants.

- ¹I. S. Jacobs, *J. Appl. Phys.* **32**, Suppl. 61S (1961).
²K. L. Dudko, V. V. Eremenko, and V. M. Fridman, *Zh. Eksp. Teor. Fiz.* **61**, 678 (1971) [*Sov. Phys. JETP* **34**, 362 (1972)].
³M. I. Kaganov and G. K. Chepurnykh, *Fiz. Tverd. Tela (Leningrad)* **11**, 911 (1969) [*Sov. Phys. Solid State* **11**, 745 (1969)].
⁴V. A. Popov and V. I. Skidanenko, *Fiz. Kondens. Sostoyaniya No. 7*, 49 (1970).
⁵V. S. Kuleshov and V. A. Popov, *Fiz. Tverd. Tela (Leningrad)* **15**, 937 (1973) [*Sov. Phys. Solid State* **15**, 652 (1973)].
⁶V. V. Eremenko, Yu. A. Popkov, and L. T. Kharchenko, *Pis'ma Zh. Eksp. Teor. Fiz.* **3**, 233 (1966) [*JETP Lett.* **3**, 149 (1966)].
⁷R. S. Meltzer and L. L. Lohr, Jr., *J. Chem. Phys.* **49**, 541 (1968).
⁸V. V. Eremenko, N. E. Kaner, Yu. G. Litvinenko, and V. V. Shapiro, *Zh. Eksp. Teor. Fiz.* **84**, 2251 (1983) [*Sov. Phys. JETP* **57**, 1312 (1983)].
⁹R. L. Melcher, *Phys. Rev. Lett.* **25**, 235 (1970).
¹⁰R. L. Melcher, *Phys. Rev. B* **1**, 4493 (1970).
¹¹A. A. Mil'ner, Yu. A. Popkov, and V. V. Eremenko, *Pis'ma Zh. Eksp. Teor. Fiz.* **18**, 39 (1973) [*JETP Lett.* **18**, 20 (1973)].
¹²J. de Gunzbourg and J. P. Krebs, *J. Phys. (Paris)* **29**, 42 (1968).

Translated by A. Tybulewicz